Life-Cycle of Structures and Infrastructure Systems – Biondini & Frangopol (Eds)

Seismic and energetic renovation of existing masonry buildings by innovative FRLM composite materials

D. Pugliese, V. Alecci, S. Galassi, A.M. Marra & M. De Stefano
University of Florence, Florence, Italy

ABSTRACT: The energy and seismic requalification of the existing building heritage is a crucial topic, usually investigated by separate approaches and procedures. In this context, the designed technologies must reflect on solutions that can be applied in redevelopment interventions from the perspective of Life Cycle Thinking. Moreover, the choice of a specific solution in the construction sector must face the rise of mechanical and energy performance levels according to the market requests, as well as the demands of a regulatory landscape increasingly focused on the principles of sustainability and LCA-based environmental impact of the entire building process.

In this framework, this research aims to design, test and implement innovative strengthening systems made of bio-composite mortar mixtures in which a high-strength fiber is embedded, covering an integrated assessment of new composite materials to reduce the seismic vulnerability of historic masonry buildings while complying with energy saving, sustainable development, and reduction of greenhouse gases emissions.

After an initial literature review outlining the progress in innovative techniques for the integrated structural and energy retrofit of existing masonry buildings, the study focuses on the applications of fibre-reinforced lime matrices (FRLM) as thermal plasters, analyzing their mechanical properties and thermo-hygrometric behaviour.

Next, a selection of thermal plasters to be used as a matrix of the innovative composite material was carried out; then, the mechanical properties were investigated through compressive and bending tests. The mortar with better mechanical properties was used to assemble composite specimens to be tested under a direct tensile test. Dynamic thermohygrometric simulations by WUFI® Pro and EnergyPlus and numerical FEM simulations using the Abaqus software were performed to check structural and thermal contributions when applied on typically arranged masonry panels of existing buildings.

The objective is to demonstrate how it is possible to provide solutions that can encourage ecological and environmental sensitivities of processes and products and define approaches for future projects to achieve sustainable targets positively.

1 INTRODUCTION

Most European masonry buildings are made in the absence of anti-seismic standards and thermal insulation requirements and do not pay attention to either structural safety or energy performance. The conservation and valorization of this heritage require a multidisciplinary approach, capable of reducing structural vulnerability by upgrading the energy performance while respecting environmental sustainability principles, from a Life Cycle Thinking perspective.

In the current literature, several methods exist to improve the thermal performance of masonry buildings (Litti et al., 2015) and for the seismic vulnerability assessment (Karantoni et al., 2012) but operate in a disjoint way.

DOI: 10.1201/9781003323020-454

In addition, only a few research projects are available on an integrated approach to evaluate new methods of structural and energetic requalification of existing masonry buildings (Giresini, Casapulla, et al., 2021; Giresini, Stochino, et al., 2021): a comparison between thermal performance and seismic capacity of different interventions on masonry structures, in terms of economic (e/m^2) and ecological (kgCO2/m^2) costs is proposed in (Mistretta et al., 2019).

The reinforcement of masonry structures is one of the most important applications for FRLM (Fiber Reinforced Lime Matrix) composite materials. The reinforcement, defined by a fibrous base, guarantees an improvement of the mechanical characteristics, while the matrix allows the application of the reinforcement to the structural system, sometimes improving the thermo-hygrometric performance also. The challenge in introducing technological solutions as innovative composite materials compatible with the organism to preserve (Battisti et al., 2018), able to increase mechanical resistance, improving the inertia and thermal transmittance, without burdening the structures, is the aim to create sustainable strategies to improve the existing masonry heritage building subjected to energy losses and earthquake loading.

This paper aims to develop one or more innovative FRLM composite materials made by a balanced bi-axial mesh of basalt fiber and thermal plasters based on natural hydraulic lime mortar. Thermal plasters are mortars for masonry that show excellent insulating characteristics (UNI EN 998-1, 2016) and can be produced using lightweight aggregates of natural origin or recycled or recyclable materials, as a starting point to reduce the environmental impact of the construction sector. The concept of environmental impact is to be understood by observing the "From Cradle to Cradle" approach, following the Life Cycle Assessment (LCA) method, to study the influence that the production process has on factors related to climate change (Napolano et al., 2015).

Starting from these premises, first, a comparative analysis of eleven thermal plasters was made to identify the one with the best performance from a mechanical, thermo-hygrometric, and environmental perspective.

The thermohygrometric properties of the thermal plasters were evaluated through dynamic simulations with the WUFI ® Pro software, while the mechanical properties were investigated through three-point bending and compression tests. The thermal plaster with the best properties was assembled with basalt fibers and tested at the laboratory under direct tension tests.

Finally, Finite element analyses with Abaqus software were performed to estimate the composite's mechanical contributions and failure mechanism.

2 ANALYSIS OF THE INORGANIC MATRICES FOR THE FRLM COMPOSITES

After a detailed study of the state of the art through an original analysis of the products present in the literature and the international market, the first part of the research work involved the identification of lime-based thermal plasters with mechanical and energetic characteristics for the rehabilitation of existing masonry buildings.

The requirements imposed on the properties of the thermal plasters were identified concerning the following parameters: 1) compressive strength σ [N/mm^2]; 2) thermal conductivity λ [W/mK].; 3) density [kg/m^3]: 4) natural aggregates; 5) recycled or recyclable aggregates.

Table 1. lists the composition of 11 selected thermal plasters declared by manufacturers on data sheets. The symbols next to the codes (Int.01- Int.11) indicate the type of compound, in particular:

- ✓ indicates that the thermal plaster is characterized by a $\sigma \simeq 1{,}50$ N/mm^2 and $\lambda \simeq 0{,}10$ W/mK;
- 🍃 indicates that the thermal plaster is made of natural materials;
- ♻ indicates that the thermal plaster is made of recycled or recyclable materials.

3 HYGROTHERMAL PERFORMANCES OF THE SELECTED MATRICES

With the purpose to investigate the one-dimensional transient hygrothermal behaviour of multilayer building components, thermodynamic simulations were performed using the

Table 1. Composition of Int.01- Int. 11 matrices.

Thermal Plaster	Compressive strength σ [N/mm²]	Thermal Conductivity λ [W/mK]	Density [kg/m³]	Binder
Int.01 ✓🍃	> 3.0	0.077	400	Natural Hydraulic Lime (NHL) 3.5
Int.02 ✓🍃♻	0.4 to 2.5	0.075	380	Natural Hydraulic Lime (NHL) 3.5
Int.03 ✓🍃	3.5 to 7.5	0.046	395	Natural Hydraulic Lime (NHL) 5
Int.04 ✓🍃	≥ 2.0	0.086	385	Natural Lime
Int.05 ✓🍃♻	2.0	0.064	365	Natural Hydraulic Lime (NHL) 3.5
Int.06 ✓🍃	2.0	0.048	380	Natural Hydraulic Lime (NHL) 3.5
Int.07 ✓🍃♻	1.5	0.104	400	Slaked Lime
Int.08 ✓🍃	0.4 to 2.5	0.0757	390	Natural Hydraulic Lime (NHL) 3.5
Int.09 ✓🍃	0.4 to 2.5	0.067	≤ 400	Natural Hydraulic Lime (NHL)
Int.10 ✓🍃	0.4 to 2.5	0.137	1300	Natural Hydraulic Lime (NHL)
Int.11 ✓🍃	0.4 to 2.5	0.057	400	Natural Hydraulic Lime (NHL) 5

WUFI ® Pro 6.5.2 software (Wärme- Und Feuchtetransport Instationär Heat and Moisture Transiency) according to UNI EN standard (UNIEN15026, 2008).

The climatic reference conditions of Florence were considered with a simulation time of ten years.

Three specific technical solutions for masonry buildings were considered for the simulation, selected from the list provided by UNI/ TR standard (UNI/TR11552, 2014) in particular:

- Mas.1: one-and-a-half brick masonry, with a thickness of 380 mm;
- Mas.2: stone masonry, with a thickness of 500 mm;
- Mas.3: sack masonry with weakly bonded filling, with a thickness of 480 mm.

In the field of seismic and energy requalification of the historical heritage, the 11 selected thermal plasters were applied on both sides of the wall considering 60 mm thick on the exterior and 40 mm thick on the interior. to investigate the hydrothermal behaviour of the different scenarios varying the thermal plasters adopted to replace the traditional plaster.

For all the investigated solutions, the simulations show that the water content inside the wall [kg/m^3] increases over the ten years: initially, the structure is not yet in dynamic equilibrium with the environment; once this equilibrium has been reached, the variations of the water content inside the wall depends on seasonal variations.

As regards the water content inside the internal plaster layer [kg/m^3], the products with the lowest annual average value are Int.01 and Int.06. Furthermore, the results obtained from the simulations carried out with Int.06 showed no water accumulation within any of the three analyzed construction types.

Figure 1. reports each configuration's thermal transmittance values [W/m^{2}K] of the three building envelope solutions Mas.1, Mas.2, and Mas.3 for the climate of Florence.

4 EXPERIMENTAL INVESTIGATION OF THE MECHANICAL PROPERTIES

The experimental campaign was carried out at the Laboratory of Materials and Structures of the University of Florence, which involved:

- bending tests for three points and uniaxial compression tests of the 11 selected thermal plasters;
- direct tensile test on basalt textile;
- direct tensile test on the FRLM composite constituted by the structural reinforcing textile embedded in the better thermal plaster from the structural and thermodynamic point of view.

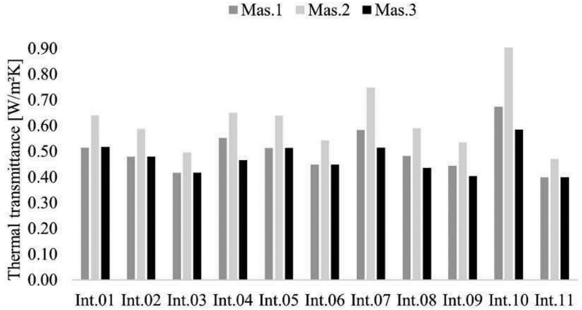

Figure 1. Comparison between the thermal transmittance values of the different configurations.

4.1 *Mechanical properties of the thermal plasters*

Three mortar specimens 40·40·160 mm^3 in size for each type of thermal plaster (Int.01-Int.11) were obtained using special standardized metal moulds and tested, after curing for 28 days in a controlled temperature room, under three-point bending tests, according to UNI standards (UNIEN1015, 2019). Then, axial compression tests on the two stumps obtained after the failure of each specimen due to the bending test were performed.

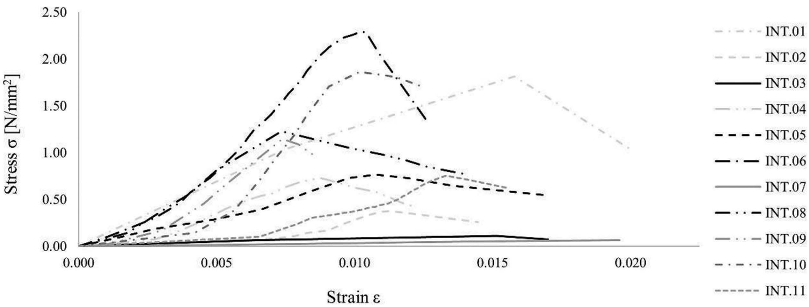

Figure 2a. a) Compressive stress-strain curves of Int.01-Int.11.

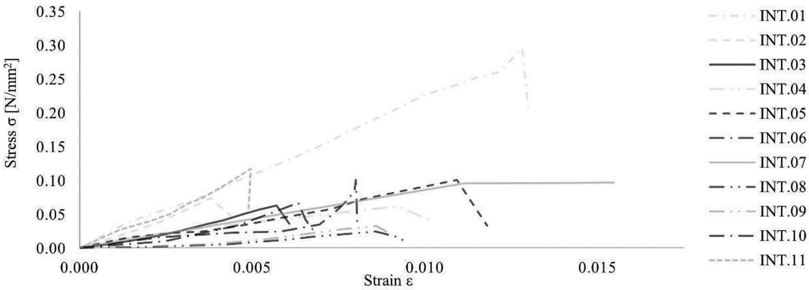

Figure 2b. b) Flexural stress-strain curves of Int.01-Int.11.

The tests were carried out under displacement control, using an universal hydraulic machine with a 600 kN hydraulic actuator. Results of the three-point bending test and compression test were summarized in Table 2 in terms of compressive strength (f_c), compressive elastic modulus (E_c), and flexural strength (f_b). Elastic modulus was calculated and evaluated between 30% and 60% of the maximum load (Alecci et al., 2019; Simões et al., 2015; Valluzzi et al., 2005) in the first linear branch of the stress-strain curves.

Compressive and flexural stress-strain curves of the texted thermal plaster specimens are plotted in Figures 2a) and 2b).

The results obtained from the experimental campaign concerning the four resistance categories of plaster mortar reported in the technical standards for the design, execution, and testing of masonry buildings (UNIEN998-1, 2016) identified the thermal plasters tested as belonging to category CS I (0.4 ÷ 2.5 N/mm^2), with an average compressive strength of 1.13 N/mm^2. For the flexural and compressive strengths, respectively, the values are in the ranges of 0.02 N/mm^2 and 0.30 N/mm^2 for flexural and 0.11 N/mm^2 and 2.49 N/mm^2 for compressive strength. Accordingly, the flexural and uniaxial compression tests show that the thermal mortar with the best compressive strength is INT.06, with a value of compressive strength equivalent to 2.46 N/mm^2. It can be noted that thermal plasters INT.06, INT.01, and INT.10 showed the highest value of compressive strength, flexural strength, and Young's modulus, respectively.

Table 2. Mechanical properties of Int.01- Int.11 matrices (laboratory results).

Thermal Plaster	Compressive strength f_c [N/mm^2]	Compressive Young's modulus [N/mm^2]	Flexural strength [N/mm^2]
Int.01	2.41	138.7	0.30
Int.02	0.38	75.9	0.07
Int.03	0.46	10.7	0.06
Int.04	0.73	132.0	0.06
Int.05	0.89	63.7	0.10
Int.06	2.49	292.5	0.27
Int.07	0.11	3.2	0.10
Int.08	1.23	222.2	0.02
Int.09	1.15	211.3	0.03
Int.10	1.86	385.1	0.07
Int.11	0.76	77.30	0.12

4.2 *Mechanical properties of the basalt textile*

The textile used for the reinforcement of the new FRLM composite is a balanced bi-axial mesh made of special basalt fiber and stainless-steel micro threads.

Direct uniaxial tensile tests investigated the mechanical properties of the basalt textile, performed under controlled displacement by an universal testing machine equipped with a 600 kN load cell (Barducci et al., 2020). The load was applied with a rate of 0.25 mm/min. The tests were carried out according to the ASTM Standard (ASTMD3039/D3039M17, 2017).

Specifically, four basalt textile specimens consisting of one (1BT), two (2BT), three (3BT), and four (4BT) longitudinal multifilaments were prepared and tested.

The tensile strength ftf was obtained as shown in Equation 1:

$$f_{tf} = F_{max}/A_f \tag{1}$$

where F_{max} is the maximum load value, $A_f = n \cdot b_f \cdot t_f$ represents the equivalent cross-sectional area of the fiber, n is the number of longitudinal fiber bundles of the specimen, bf is the pitch between the bundles of fibers, and t_f is the equivalent thickness.

Young tensile modulus E_{tf} was evaluated in the first linear branch of the stress-strain curve.

Table 3. Mechanical properties of basalt textile.

Specimen	Tensile strength f_{tf} [N/mm^2]	Tensile Young's modulus E_{tf} [N/mm^2]	Ultimate strain ε_{tf}
BT	865	60487	0.017

4.3 *Mechanical properties of the composite material*

Basalt textile was embedded in the matrix Int.06, and six coupons labelled INT06_1-6, 500·65·10 mm^3 in size, after curing for 28 days at room temperature, were tested under direct tension. Two steel plates bolted with a pressure controlled by a torque wrench were used (Figure 3). The tests were performed in displacement control, with a 0.2 mm/min rate, using an universal machine with a 600 kN load cell.

The local displacements were captured using a proper extensometer 50 mm axial gauge length positioned in the middle of each specimen (Figure 4.).

Figure 5 shows the direct tensile stress and strain response curves obtain in a direct tensile test. As visible, the tested coupons showed similar mechanical behaviour for INT06_1 and INT06_4, and for INT06_3 and INT06_5 where after reaching maximum stress, the curves show a constant descending trend. When the peak load was reached, the failure of a multifilament of the basalt textile occurred.

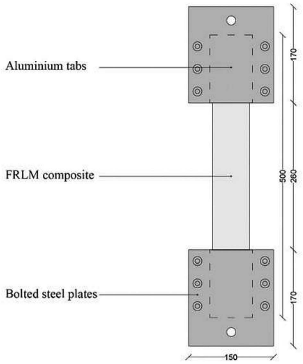

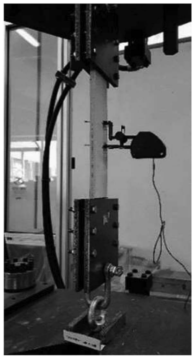

Figure. 3. FRLM direct tensile test set-up (dimension in mm). Figure 4. Tensile test on INT06_1.

The increase of the existing cracks characterized the post-peak softening branch, and the formation of new cracks and specimens highlighted large displacements without a high increase in applied load.

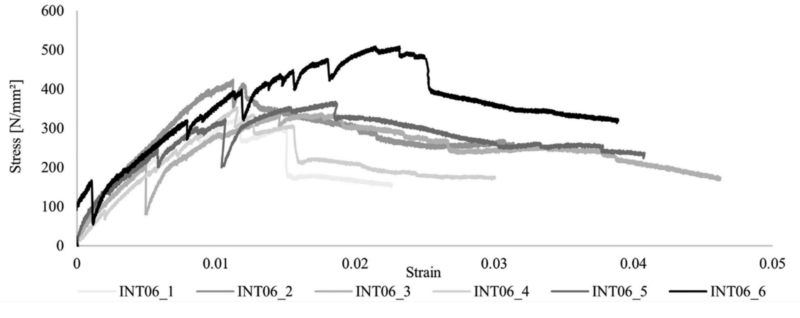

Figure 5. Stress-strain curves of the six samples INT06_1 to INT06_6.

In terms of maximum load Fmax, tensile strength f_r, Young's modulus E, and maximum deformation εr, the results are reported in Table 4.

5 FINITE ELEMENT MODELLING

Numerical analyses were carried out using Abaqus CAE software to simulate the behaviour of a non-reinforced (NRM) and a reinforced (RM) masonry wall subjected to a diagonal

Table 4. Mechanical properties of the composite material.

Coupon	F_{max} [N]	f_r [N/mm^2]	E [N/mm^2]	ε_t
INT06_1	681	327	36310	0.01
INT06_2	881	424	66577	0.01
INT06_3	704	338	34718	0.02
INT06_4	735	353	44960	0.01
INT06_5	764	367	48250	0.02
INT06_6	1059	509	52920	0.02
Average value	804	386	47289	0.015

compression test, conducted according to ASTM standards (ASTME519-07, 2010). Three parts characterize the NRM model, i.e., a brick masonry panel 1200·1200·120 mm^3 in size and two steel plates fixed at the two corners of the diagonal coinciding with the load direction (Figure 6a). The steel plate on the top distributes the load on a larger surface, avoiding the concentration of compression stresses; horizontal and vertical translational constraints are located at the base of the bottom plate. Regarding the RM, model, the FRLM composite was applied at each side (with a thickness of 15 mm) of the masonry panel by considering an isotropic linear elastic behaviour (Figure 6b).

Figure 6. a) Mesh configuration of the NRM model b) Mesh configuration of the RM model.

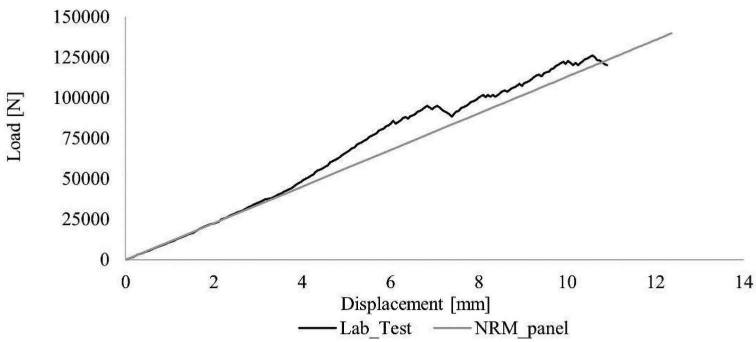

Figure 7. Comparison of the experimental and numerical results.

The steel plates were modelled with a linear elastic isotropic material, characterized by Young's modulus equal to 210000 N/mm^2 and a Poisson ratio of 0.30.

A first analysis was carried out for the NRM model, characterized by a linear elastic behaviour with Young's modulus and Poisson ratio defined to match the results of the experimental shear tests conducted previously by the Authors (Alecci, Fagone, Rotunno, & De Stefano, 2013).

Figure 7 compares the numerical and the experimental results in load-displacement evaluated at the top of the tested brick masonry panel.

Once the linear elastic analysis had been carried out, the masonry panel was studied with a nonlinear behaviour (NL_NRM), using the "concrete damage plasticity" (CDP) model implemented in Abaqus CAE, adequately calibrated according to experimental tests conducted by the authors (Alecci, De Stefano, Luciano, Marra, & Stipo, 2020). Regarding the analyses on the nonlinear FEM, they are not reported since they are still in progress.

6 CONCLUSIONS

Through a theoretical-experimental analysis, based on data in the literature and materials on the market, it was found that the identification of thermal plasters compatible with the masonry substrate to be reinforced, and characterized by good mechanical as well as thermal properties, is a crucial step for the design of innovative composite materials to be used for the energy and structural upgrading of the historic building, in compliance with the instances of compatibility, sustainability, and reversibility (Romano et al., 2021).

The results reported in this paper show that Int.01, Int.06, and Int.10 mortars have good mechanical behaviour in terms of compressive strength, flexural strength, and Young's modulus values.

Regarding the energetic performance, it was observed that the walls with the lowest thermal transmittance were those retrofitted with Int.06, applied on both sides to both sides of the wall.

Finally, the INT.06 product represents the ideal matrix from both points of view and can be considered a good solution to regenerate the thermohygrometric performances of the historical envelopes, without changing their mechanical and aesthetic features.

The next step of the research will involve the seismic retrofit of masonry panels strengthened with such a composite by a nonlinear FEM analysis while enlarging the list of thermal plaster mixtures evaluated as potential matrices of the FRLM composites.

REFERENCES

Alecci, V. et al., 2020. Numerical Investigation on the Use of Flat-Jack Test for Detecting Masonry Deformability. Journal of Testing and Evaluation.

Alecci, V., Fagone, M., Rotunno, T. & De Stefano, M., 2013. Shear strength of brick masonry walls assembled with different types of mortar. *Construction and Building Materials*, Volume 40, pp. 1038–1045.

Alecci, V. et al., 2019. Estimating elastic modulus of tuff and brick masonry: A comparison between on-site and laboratory tests. *Construction and Building Materials*, Volume 204, pp. 828–838.

ASTMD3039/D3039M17, 2017. Standard Test Method for Tensile Properties of Polymer Matrix Composite Materials, (West Conshohocken, PA: ASTM International).

ASTME519-07, 2010. Standard Test Method for Diagonal Tension (Shear) in Masonry. Assemblages.

Barducci, S. et al., 2020. Experimental and Analytical Investigations on Bond Behavior of Basalt-FRCM Systems. *Journal of Composites for Construction*, Volume 24.

Giresini, L., Paone, S. & Sassu, M., 2020. Integrated Cost-Analysis Approach for Seismic and Thermal Improvement of Masonry Building Façades. *Buildings*.

Romano, R. et al., 2021. Innovative and eco-compatible materials for the regeneration of the historical buildings located in the med area. *CEES 2021*, pp. 1–8.

Simões, A., Bento, R., Gago, A. & Lopes, M., 2016. Mechanical Characterization of Masonry Walls With Flat-Jack Tests. *Experimental Techniques*, 40(3), pp. 1163–1178.

Triantafillou, T. C., Karlos, K., Kefalou, K. & Argyropoulou, E., 2017. An innovative structural and energy retrofitting system for URM walls using textile reinforced mortars combined with thermal insulation: Mechanical and fire behavior. *Construction and Building Materials*.

UNI/TR11552, 2014. *Opaque envelope components of buildings - Thermo-physical parameters*.

UNIEN1015, 2019. *Test methods for masonry mortars. Part 11: Determination of flexural and compressive strength of hardened mortar*.

UNIEN15026, 2008. *Hygrothermal performance of building components and building elements - Assessment of moisture transfer by numerical simulation*.

UNIEN998-1, 2016. Specification for mortar for masonry - Part 1: Rendering and plastering mortar.

Valluzzi, M. R., Binda, L. & Modena, C., 2005. Mechanical behaviour of historic masonry structures strengthened by bed joints structural repointing. *Construction and Building Materials*, 19(1), pp. 63–73.